

The Cosmological Origin of Disk Galaxy Scaling Laws

Matthias Steinmetz

*Steward Observatory, University of Arizona, 933 N Cherry Ave,
Tucson, AZ 85721 USA*

Julio Navarro

*Department of Physics and Astronomy, University of Victoria, Victoria,
BC V8P 1A1, Canada*

Abstract.

We discuss possible origins of scaling laws relating structural properties of disk galaxies within the context of hierarchically clustering theories of galaxy formation. Using gasdynamical simulations that incorporate the effects of star formation we illustrate these global trends and highlight the difficulties faced by models that envision disk galaxies as the final outcome of a hierarchical sequence of merger events. In particular, we focus on the cosmological origin of the Tully–Fisher relation, and argue that this correlation between the total luminosity and rotation speed of disk galaxies is a natural result of the approximately scale free formation process of the massive halos they inhabit. Although the slope and scatter of the Tully–Fisher relation can be readily reproduced in hierarchical formation scenarios, the observed zero-point of the relation is inconsistent with simulations of galaxy formation in Cold Dark Matter universes, a difficulty that can be traced to the high central mass concentration of dark halos formed in this cosmogony. This result indicates that substantial revision to the new “standard” model of structure formation (Λ CDM) may be needed in order to accommodate observations on the scale of individual disk galaxies.

1. Introduction

It is well known that the dynamical and structural properties of galaxies obey a number of well defined scaling laws. Examples of these correlations include (i) the Tully-Fisher (henceforth TF) relation relating the luminosity and rotation speed of disk galaxies, (ii) the Fundamental Plane linking the surface brightness, velocity dispersion, and size of elliptical galaxies, and (iii) Schmidt’s law, which relates gas surface density and star formation rates of spiral galaxies. While some of these scaling laws can be deduced from fairly basic physical principles, such as the virial theorem, in general the details of their origin are only poorly understood.

In this contribution we report on recent progress identifying a cosmological origin of the TF relation through high resolution numerical experiments.

The present paper complements studies based on analytical and semianalytical models reported elsewhere in this volume (see, e.g., contributions by F. van den Bosch and by H. Mo) and improves upon earlier work on this topic by, e.g., Evrard et al. (1994), Tissera et al. (1997), Elizondo et al. (1999), and Steinmetz & Navarro (1999). In §2 we summarize the main features of our simulation techniques and describe the results of our simulations while §3 discusses our findings. Section 4 summarizes our main results and conclusions.

2. Numerical Simulations

2.1. The Numerical Method

The simulations were performed using GRAPESPH, a code that combines the Smoothed Particle Hydrodynamics (SPH) approach to numerical hydrodynamics with a direct summation N-body integrator optimized for the special-purpose hardware GRAPE (Steinmetz 1996). GRAPESPH is fully Lagrangian and highly adaptive in space and time through the use of individual particle smoothing lengths and timesteps. It is thus optimally suited to study the formation of highly non-linear systems such as individual galaxy systems in a cosmological context. The code used for the simulations described in this paper include the self-gravity of gas, stars, and dark matter, a full 3D hydrodynamical treatment of the gas, radiative and Compton cooling, and a simple recipe for transforming gas into stars and for incorporating the feedback of mass and energy into the gaseous component driven by evolving stars.

2.2. Star Formation and Feedback Recipes

Star formation is modeled by creating new collisionless “star” particles in Jeans-unstable, collapsing regions at a rate given by $\dot{\rho}_\star = c_\star \rho_{\text{gas}} / \max(\tau_{\text{cool}}, \tau_{\text{dyn}})$. Here ρ_{gas} is the local gas density, τ_{cool} and τ_{dyn} are the local cooling and dynamical timescales, respectively, and c_\star is a star formation “efficiency” parameter. After formation, “star” particles are only affected by gravitational forces, but they devolve energy to their surroundings in a crude attempt to mimic the energetic feedback from supernovae: 10^{49} ergs (per M_\odot of stars formed) are injected into their surrounding gas about 10^7 yrs after their formation. This energy is invested mostly in raising the internal energy (temperature) of the gas, but a fraction f_v is invested in modifying the bulk motion of the gas surrounding star forming regions. For details, see Steinmetz & Navarro (1999) and references therein.

The star formation and feedback recipe described above involves two free parameters: the star formation parameter c_\star and the feedback parameter f_v . We have performed three sets of simulations with various star formation and feedback parameters; (i) $f_v = 0$, $c_\star = 0.05$, (ii) $f_v = 0.2$, $c_\star = 0.05$, and (iii) $f_v = 0.2$, $c_\star = 1.00$. Each set includes about 35 galaxies with circular velocities between 80 and 400 km s⁻¹. Each of these galaxies has, at $z = 0$, at least 3000 star particles. For these three parameter choices, Kennicutt’s (1998) relation between the HI surface density and the star formation rate per unit area (Schmidt’s law) is roughly reproduced in isolated galaxy test cases; however, the gas fractions of $z = 0$ galaxy models vary substantially (by more than a factor of 3) for the three different parameter choices.

2.3. The Cosmological Model

The cosmological models we investigate are two flavors of the Cold Dark Matter (CDM) scenario; the traditional standard CDM model (“sCDM”, characterized by $\Omega = 1$, $h = 0.5$, $\Omega_b = 0.0125 h^{-2}$, and $\Lambda = 0$) and a flat CDM model with an non-zero cosmological constant (Λ CDM; with parameters $\Omega = 0.3$, $h = 0.7$, $\Omega_b = 0.0125 h^{-2}$, and $\Lambda = 0.7$). Both models are normalized to reproduce the observed number density of massive galaxy clusters at $z = 0$.

For each cosmological model and for each set of star formation and feedback parameters, we identify ≈ 35 dark matter halos and measure the circular velocity of the central disks at a fiducial radius $r_{\text{gal}} = 15 (V_{200}/220 \text{ km s}^{-1}) h^{-1}$ kpc, where V_{200} is the circular velocity of the system at the “virial radius” where the mean inner overdensity is 200 times the critical density for closure. The radius r_{gal} contains most of the baryonic component of the luminous galaxy and is much larger than the numerical softening; galaxy properties computed at r_{gal} are rather insensitive to numerical limitations. The circular velocity profiles of simulated galaxies are approximately flat near the center; indeed, the circular velocity at $r_{\text{gal}} = 15 (V_{200}/220 \text{ km s}^{-1}) h^{-1}$ kpc and at $3.5 (V_{200}/220 \text{ km s}^{-1}) h^{-1}$ kpc (corresponding to about 2 disk scale lengths, the radius at which observed rotation velocities are typically measured) differ by less than 20% in all the systems we consider.

2.4. A numerical Tully–Fisher relation

Figure 1 (left panel) compares observational data with the simulated TF relations obtained for two different feedback prescriptions in the sCDM model. Corresponding data for the Λ CDM scenario are shown in figure 2 (left panel, open circles correspond to $c_* = 0.05$ and $f_v = 0$). This comparison illustrates a number of interesting features.

- The slope of the numerical TF relation is in good agreement with the observed TF relation, independent of the cosmological model and of the star formation and feedback description. Only for very low rotation speeds ($V_{\text{rot}} \lesssim 100 \text{ km s}^{-1}$) a somewhat shallower slope can be observed in the case of a kinetic feedback model. Also in agreement with observations, the numerical TF relations in other bands (not shown) show a systematic steepening from the blue to the red band passes (Steinmetz & Navarro, 1999).
- The scatter of the numerical TF relation is quite small. The rms scatter in the I-band is only 0.25 mag, even smaller than the observed scatter of ~ 0.4 mag. This must be so if our results are to agree with observations: scatter in the models likely reflects the intrinsic dispersion in the TF relation, whereas the observed scatter includes the additional contribution from observational errors. The small scatter is somewhat surprising, since the fraction of baryons that cool and settle into the disk varies substantially between individual halos.
- There is a serious discrepancy in the zero point of the TF relation. At a given circular velocity, simulated galaxies are about 2 magnitudes (in I)

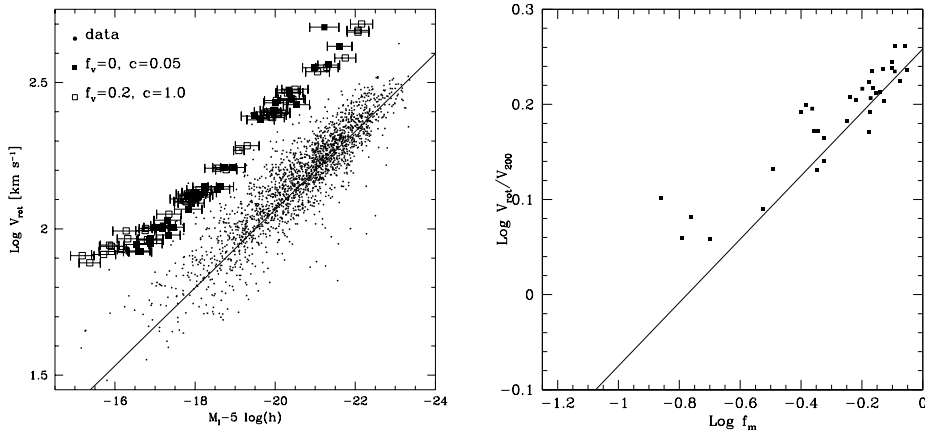


Figure 1. Left: I band Tully–Fisher relation at $z = 0$ for an $\Omega = 1, \Lambda = 0$ CDM scenario. Error bars in the simulated dataset span the difference in magnitude that results from adopting a Salpeter or a Scalo IMF. Right: ratio of the circular velocities at r_{gal} and at the virial radius (see text for definitions) versus the fraction of baryons that have cooled, settled into the central disk and turned into stars. The solid line corresponds to $V_{\text{rot}}/V_{200} \propto f_m^{1/3}$.

too dim. The discrepancy is rather insensitive to the cosmological model and/or adopted star formation and feedback recipe.

3. TF Relation: Observations vs Numerical Experiments

In order to further our insight into the meaning of the successes and failures of our TF modeling we shall focus on the following questions. (i) Why is the simulated TF slope in such good agreement with observations? (ii) Why is the scatter in the numerical TF relation so small, in particular considering that the fraction of baryons inside the virial radius effectively accreted into the central galaxy, f_m , varies significantly from halo to halo? (iii) Why is the zero-point of the numerical relation in disagreement with observations?

3.1. The Slope

The slope of the numerical TF relation can be understood as a direct consequence of the cosmological equivalence between mass and circular velocity (see, e.g., Mo, Mao & White 1998). This equivalence is a consequence of the finite age of the universe, which imposes a maximum radius (approximately equal to the “virial radius”) from where matter can accrete to form a galaxy (for an alternative view in which the slope is derived as a result of self-regulated star formation in disks of different mass, see Silk 1997). At $z = 0$, the circular velocity at the virial radius (V_{200}) and its enclosed mass (M_{200}) are then equivalent measures of the

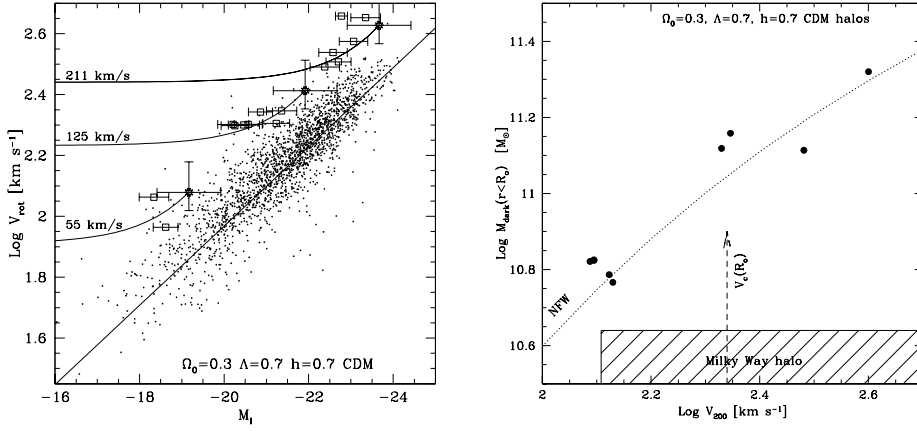


Figure 2. Left: Right: I-band TF relation at $z = 0$ for $\Omega = 0.3, \Lambda = 0.7$. See text for details. Right: Dark mass enclosed within a radius $R_o = 8.5$ kpc, the Sun’s distance from the center of the Milky Way, versus the circular velocities of Λ CDM halos. The shaded region highlights the allowed parameters of the dark halo surrounding the Milky Way. The filled circles show the loci of Λ CDM halos as determined from high-resolution N-body simulations. The dotted line is the circular velocity dependence of the dark mass expected inside R_o for halos that follow the density profile proposed by NFW.

system’s mass related by

$$M_{200} = 2.33 \times 10^5 \left(\frac{V_{200}}{\text{km s}^{-1}} \right)^3 h^{-1} M_{\odot}. \quad (1)$$

Given this scaling, if disk rotation speeds are proportional to the circular velocity of their surrounding halos ($V_{rot} \propto V_{200}$) and disk (stellar) masses are proportional to the mass of the halos, $M_{disk} \propto M_{200}$, then one expects $L_I = \Upsilon_I^{-1} M_{disk} \propto V_{rot}^3$, under the assumption that the I-band stellar mass-to-light ratio, Υ_I , does not vary dramatically with galaxy luminosity. Such velocity dependence is similar to that of the observed TF relation, which can be approximated by

$$L_I \approx 2.4 \times 10^{10} \left(\frac{V_{rot}}{200 \text{ km s}^{-1}} \right)^3 h^{-2} L_{\odot}, \quad (2)$$

(see solid lines in the left panels of Figures 1 and 2). Assuming that the baryon density parameter is $\Omega_b \approx 0.0125h^{-2}$, as suggested by Big Bang nucleosynthesis studies of the abundance of the light elements (Schramm & Turner, 1998), the fraction of baryons transformed into stars in disk galaxies is given by,

$$f_m \approx \Upsilon_I \Omega_0 h \left(\frac{V_{rot}}{V_{200}} \right)^3. \quad (3)$$

Under the assumption that $V_{rot} = V_{200}$ and adopting $\Upsilon_I \sim 2$ in solar units, as suggested by stellar population synthesis models, eq. 3 implies that almost

all the baryons in sCDM halos have been transformed into stars, but that only about 40% have suffered that fate in Λ CDM halos (see Navarro & Steinmetz, 2000a,b for details). The low efficiency in the transformation of baryons into stars (especially in the case of Λ CDM halos) should be contrasted with the relatively large specific angular momenta of disks and halos of similar circular velocities. Although only 40% of the available baryonic mass is collected at the center of a Λ CDM halo, analytical estimates indicate that those baryons are able to acquire as much as $\sim 100\%$ of the specific angular momentum of the halo (Mo et al 1998). This appears to indicate that disk galaxies are assembled preferentially from high-angular momentum content gas, a feature that has proved rather difficult to reproduce in numerical simulations (see, e.g., Navarro & Steinmetz 1997).

3.2. The Scatter

In the context of the model described in §3.1, a number of possible sources of scatter in the TF relation may be identified; variations in the ratio between disk rotation speed and halo circular velocity, systematic variations in the stellar mass-to-light ratio of galaxies with similar rotation speeds, and disparities in the fraction of baryons f_m that cool and settle into the disk. The latter can be easily measured in our simulations, and is found to vary by almost a factor of 2 from galaxy to galaxy. Taken at face value, this would imply a scatter in the TF relation of approximately 0.8 mag, larger than the observed value of ~ 0.4 mag. However, as discussed above, this is not the case; the measured scatter of the numerical TF relation is actually significantly smaller than the observed one.

The small scatter in the numerical TF relation introduced by variations in f_m results from a tight relation between f_m and the rotation velocity of the galactic disk. The higher the fraction of baryons that assemble into the central stellar disk the higher the luminosity of the galaxy, but also the higher its circular velocity, due to the gravitational contribution of this additional material. This effect is further amplified by the dark matter’s response to this extra gravitational pull. This is illustrated in Figure 1 (right panel), which shows the ratio of disk rotation speed (measured at r_{gal}) and the virial velocity, V_{200} , versus f_m . The velocity ratio scales approximately as $f_m^{1/3}$ (shown as a solid line), indicating that variations in the star to dark matter fraction result in shifts parallel to the TF relation, adding very little scatter to the original relation. The scatter in the numerical TF relation is thus largely the result of (small) differences in the assembly and star formation history of the halos that these galaxies inhabit.

3.3. The Zero Point

Although the slope and scatter of the numerical TF relation compare favorably with observation, simulated galaxies are, at given rotation speed, almost two magnitudes fainter than observed. This serious discrepancy seems to be associated with the large concentration of dark matter near the center of Cold Dark Matter halos. When these large amounts of dark matter are added to the substantial mass in baryons needed to build a bright spiral the rotational speeds that result are inconsistent with the observed TF relation.

This is shown in Figure 2 (left panel), where we show where hypothetical disk galaxies built at the center of three representative dark halos of different

circular velocity would lie in the $M_I - V_{\text{rot}}$ plane. The three solid curves in this panel illustrate the loci of galaxies of different luminosity in this plane, under the assumption of constant stellar mass-to-light ratio ($\Upsilon_I = 2$ in solar units). Along each curve (from left to right) the stellar mass of the disk varies from \sim zero to the maximum value compatible with the baryonic content of the halo, the rightmost point of each curve. As the disk mass increases, each hypothetical galaxy moves from left to right across the plot. When the disk mass becomes comparable to the dark mass inside the optical radius of the galaxy the curve inches upwards and becomes essentially parallel to the observed TF relation. Because of this, even under the extreme assumption that galaxies contain *all* available baryons in each halo, simulated disks are almost two magnitudes fainter than observed.

Increasing the baryonic mass of a halo further has virtually no effect on this conclusion, since in this case model galaxies would just move further along paths approximately parallel to the TF relation. As mentioned above, the main reason for the discrepancy is the large central concentration of dark matter in CDM halos. This is shown in Figure 2 (left), where the circular velocity in the inner few kpc of a $V_{200} = 125 \text{ km s}^{-1}$ halo contributed by the dark matter *alone* is shown to be of order 170 km s^{-1} (see middle solid line in this panel). Such large velocities only increase further as a result of the assembly of the luminous component, leading to the large zero-point disagreement observed in the left panels of Figures 1 and 2. Therefore, unless one (or more) of the assumptions above is grossly in error, disk galaxies assembled at the center of halos formed in the cosmological models we explored (sCDM and Λ CDM) cannot match the observed Tully–Fisher relation.

Perhaps the most uncertain step in this argument is the stellar mass-to-light ratio adopted for the analysis. The horizontal “error bar” shown on the starred symbols in Figure 2 (left) illustrates the effect of varying the I -band mass-to-light ratio by a factor of two from the fiducial value of 2 in solar units. This is not enough to restore agreement with observations, which would require $\Upsilon_I \sim 0.4$, a value much too low to be consistent with standard population synthesis models. The vertical “error bars” illustrate the effect of varying the “concentration” of each halo by a factor of two. Even with this large variation in halo structure, the model disks fail to reproduce the observations.

The only way to collect a massive disk galaxy without increasing V_{rot} significantly over V_{200} is to have dark halos that are less centrally concentrated than those formed in the sCDM or in the Λ CDM scenario. We note that this problem is unlikely to be solved just by adjusting cosmological parameters of the CDM model. The combination of parameters needed to reproduce the present-day abundance of galaxy clusters is such that the central densities of galaxy-sized dark halos is approximately independent of Ω_0 and of the value of H_0 (Navarro 1999). This explains why there is no noticeable difference in the zero point of the sCDM and Λ CDM simulated TF relations (Figures 1 and 2, respectively). The difficulties may be even more generic: modifications to the CDM scenario that may potentially solve the problems described here (e.g. tilted power spectra, additional hot dark matter, annihilating dark matter, to name a few) will delay the formation epoch of dark matter halos to lower redshift. This may hinder the formation of massive galaxies at high redshift, at odds with the mounting

evidence that such galaxies are fairly common at $z \gtrsim 3$ (see, e.g., Steidel et al 1998).

3.4. Application to the Milky Way halo

The conclusion that cold dark matter halos are too centrally concentrated can be independently checked by using observations of the dynamics of the Milky Way that constrain the total dark mass within the solar circle (R_o). A direct estimate can be made by assuming that the halo is spherically symmetric and by combining the local density of the disk derived from ‘‘Oort limit’’ analysis with the IAU-sanctioned values of $R_o = 8.5$ kpc and $V_{\text{rot}}(R_o) = 220$ km s $^{-1}$. This implies that the dark mass within R_o cannot exceed $M_{\text{dark}}(r < R_o) = 5.2 \times 10^{10} M_{\odot}$ (Navarro & Steinmetz 2000a).

Figure 2 (right panel) compares this value with dark masses inside 8.5 kpc measured directly from N-body simulations of Λ CDM halos. The conclusion is clear: halos with $V_{200} \approx 220$ km s $^{-1}$ have on average *three times* more dark matter inside R_o than allowed by observations. Only halos with $V_{200} < 100$ km s $^{-1}$ are eligible as hosts of the Milky Way, but they can be ruled out on the basis of the total (baryonic) mass of the luminous component, $M_{\text{disk}} \approx 6 \times 10^{10} M_{\odot}$. This mass implies a strict minimum halo mass through the universal baryon fraction of the universe, which, expressed in terms of circular velocity, indicates that the halo of the Milky Way must have $V_{200} \gg 130$ km s $^{-1}$. As illustrated in Figure 2 (right), these constraints on the halo of the Milky Way are inconsistent with the results of N-body simulations.

4. Summary and Conclusions

We have studied the formation of disk galaxies in hierarchical clustering scenarios using high resolution hydrodynamical simulations that include the effects of star formation and supernova feedback. We report here on our contribution to understanding the cosmological origin of disk galaxy scaling laws and, in particular, of the Tully–Fisher relation. Our findings can be summarized as follows.

- Adopting star formation recipes that match observational constraints (e.g. Kennicutt’s law), the slope and scatter of the TF can be easily reproduced in such numerical simulations. The slope of the I-band TF relation is essentially determined by cosmological equivalence between the mass and the circular velocity of dark matter halos. Variations in the star formation history as a function of galaxy mass only introduces a slight modulation in this slope, resulting in shallower slopes in the bluer pass bands.
- The tightness of the TF relation and its weak sensitivity to the star formation and feedback prescription is largely the result of the kinematic response of the dark matter halo to changes in the fraction of baryons that cool and settle in the central disk. The increase in the rotation velocity of the galaxy due to the self gravity of the disk and to the contraction of the dark matter halo scales in such a way that, for relevant baryon fractions, leads to displacements parallel to the TF relation, so that variations in the

disk mass assembled within each dark halo affect the slope of the relation only weakly and introduce little additional scatter.

- Despite the success in reproducing its slope and scatter, galaxies formed inside cold dark matter halos exhibit a substantial zero-point offset from the observed TF relation. This is due to the large central concentrations of simulated dark matter halos, which, we show, are also in disagreement with dynamical evidence on the structure of the Milky Way's halo.

Although our conclusions are strictly valid for the two cosmological models we have investigated (sCDM and Λ CDM) they are likely to extend to all Cold Dark Matter models normalized to reproduce the observed abundance of massive galaxy clusters. This implies that the discrepancies we highlight here signal that the Cold Dark Matter paradigm, so successful at reproducing observations on large scales, may actually be unable to accommodate the constraints placed by detailed dynamical studies of individual galaxies. A thorough revision of the validity and applicability of the Cold Dark Matter scenario on the scale of individual galaxies seems warranted.

References

- Elizondo, D., Yepes, G., Kates, R., Müller, V., Klypin, A. 1999, *ApJ*, **515**, 525
Evrard, A.E., Summers, F.J., Davis, M., 1994, *ApJ*, **422**, 11
Kennicutt, R.C., 1998, *ARA&A*, **36**, 189. *ApJ*, **513**, 555
Mo, H.J., Mao, S., & White, S.D.M. 1998, *MNRAS*, **295**, 319
Navarro, J.F. 1999, *ApJ*, submitted (astro-ph 9807084)
Navarro, J.F., Frenk, C.S., & White, S.D.M. 1997, *ApJ*, **490**, 493
Navarro, J.F., Steinmetz, M. 1997, *ApJ*, 478, 13
Navarro, J.F., Steinmetz, M. 2000a, *ApJ*, in press
Navarro, J.F., Steinmetz, M. 2000b, *ApJ*, in preparation
Schramm, D.N., Turner, M.S. 1998, *Rev.Mod.Ph.* 70, 303
Silk, J. 1997, *ApJ*, **481**, 703
Steidel, C.C., Adelberger, K.L., Dickinson, M., Giavalisco, M., Pettini, M., Kellogg, M. 1998, *ApJ*, **492**, 428
Steinmetz, M. 1996, *MNRAS*, **278**, 1005
Steinmetz, M., Navarro, J.F. 1999, *ApJ*, **513**, 555
Tissera, P.B., Lambas, D.G., & Abadi, M.G. 1997, *MNRAS*, **286**, 384
White S. D. M., Navarro J. F., Evrard A. E., & Frenk C. S. 1993, *Nat*, 366, 429